The excited states decay of the A-T DNA: a PCM/TD-DFT study in aqueous solution of the (9-methyl-adenine)$_2$·(1-methyl-thymine)$_2$ stacked tetramer: Supporting Information

F. Santoro[+], V. Barone[++], R. Improta[‡†,*]

August 25, 2009

+ Istituto per i Processi Chimico-Fisici - CNR, Area della Ricerca del CNR Via Moruzzi,1 I-56124 Pisa, Italy

++ Scuola Normale Superiore di Pisa, P.zza dei Cavalieri 7, I-56126 Pisa, Italy

‡ Istituto di Biostrutture e Bioimmagini -CNr, Via Mezzocannone 16, I-80134 napoli, Italy

† Dipartimento di Chimica and INSTM, Università Federico II, Complesso Monte S. Angelo, via Cintia, I-80126 Napoli, Italy,

*e-mail:robimp@unina.it

1 Computational details

Our analysis has been performed by using PBE0 [1,2], M052X[3] and CAM-B3LYP[4,5] functionals. Whenever not explicitly stated, ground state geometry optimizations have been performed in aqueous solution at the PCM/PBE0/6-31G(d) level, including bulk solvent effects by the polarizable continuum model (PCM)[6,7].

The excited states have been characterized by computing their electric dipole moment, the formal charge present on each atom and on each m monomer ($\mathbf{Q}_m$), and the quantities $\mathbf{v}_m^n$

$$\mathbf{v}_m^n = \sum_{i=1\rightarrow N} |q_i^n - q_i^0| \tag{1}$$

where q_i^n is the Mulliken atomic charge of the i atom in the n electronic state (q_i^0 are the Mulliken charges in the ground state) and the label m ($m = 1, \ldots, 4$) denotes the monomer considered (containing $1 \rightarrow N$ atoms). The values v_m^n (computed assigning the hydrogen atoms' charges to the heavy atom they are bound to) provides an estimate of the involvement of a given monomer in the n electronic transition, being close to 0 if the Molecular Orbitals (MO) of that monomer are not involved in the n electronic transition. When not explicitly stated this analysis has been performed by using the 6-31G(d) basis set.

A more detailed discussion of our computational approach and of its reliability can be found in the following sections.

All the calculations have been performed by a development version of the Gaussian Program.[8]

1.1 Density functionals

PBE0[1] is a hybrid functional, in which the spurious self-interaction is partly cured by hybridization with Hartree-Fock exchange. In PBE0 the amount of exact exchange has been determined in order to fulfill a number of physical conditions, without resorting to any fitting procedure.[1] Besides its good performances in the study of nucleobases (see the following sections), TD-PBE0[2]

excitations energies are usually more accurate than those delivered by other commonly used hybrid functionals (e.g. B3LYP), since the fulfillment of the Levy condition and the Lieb-Oxford bound leads to a fairly accurate description of low density/high-gradient regions.[2] Furthermore, despite the absence of adjustable parameters, PBE0 has shown to provide a reliable description of conformational equilibria [9] and of excited states in biological systems,[10] as well as an overall degree of accuracy comparable with that of the best last generation functionals.[11,12] Finally, it is noteworthy that the PCM/TD-PBE0 excited state geometries and frequencies computed in the condensed phase for several different organic molecules are in remarkable agreement with their experimental counterparts.[13−15]

M052X[3] is a recently developed functional based on simultaneously optimized exchange and correlation contributions both including kinetic energy density, which allows a treatment of dispersion interactions and charge transfer transitions more reliable than that provided by previous density functionals.[16]

CAM-B3LYP[4] combines the hybrid qualities of B3LYP and the long-range correction proposed by Hirao et coll.[5] and it is particularly accurate in describing CT transitions.

1.2 Solvation Model

Bulk solvent effects on ground and excited states have been taken into account by means of the latest versions of the Polarizable Continuum Model (PCM), by using the default PCM model in Gaussian (referred to in the literature as IEF-PCM or IVC-PCM).[6] In this model the solvent, represented by an homogeneous dielectric, is polarized by the solute, placed within a cavity built as the envelope of spheres centered on the solute atoms. In our case the cavity has been built according to the UAO model (UATM model [17] using UFF radii). When discussing solvent effects on absorption spectra it is useful to define two limit situations, usually referred to as non-equilibrium (*neq*) and equilibrium (*eq*) time-regimes.[6,7] In the former case, only solvent electronic polarization (fast solvent degrees of freedom) is in equilibrium with the excited state elec-

tron density of the solute, whereas nuclear degrees of freedom (slow solvent degrees of freedom) are equilibrated with the ground state electron density. On the contrary, the equilibrium regime is reached when both fast and slow degrees of freedom are equilibrated with the excited state electron density. The solvent reaction field in the non-equilibrium regime depends in the PCM formalism on the dielectric constant at optical frequency (ϵ_{opt}, usually related to the square of the solvent refractive index n, $\epsilon_{opt} = n^2$, for water 1.776). PCM equilibrium solvation is instead ruled by the static dielectric constant (ϵ, for water 78.39). In order to calculate the Vertical Excitation Energies (VEE) and to discuss the fast part of the excited state dynamics (time $<$ 200 fs) non-equilibrium solvation energies are more suitable, while the opposite would be in principle true for fluorescence energies and for the slower part of the excited state dynamics (time $>$ 1 ps). However, the $(dA_2)\cdot(dT_2)$ and $(9Me\text{-}A)_2\cdot(1Me\text{-}T)_2$ tetramers are inserted in a DNA double helix. In this system, the response of the nuclear degrees of freedom to the variation of the electron density associated to the electronic transitions is expected to be much slower than in a standard isotropic solvent. As a consequence, in order to avoid any overestimation of solvent equilibration effects, we choose to base our study mainly on the *neq* results.

Two different implementations of PCM/TD-DFT exist. The 'standard' implementation[18] is based on the Linear Response (LR) theory: it computes excitation energies directly, without using the exact excited state electron density. Our previous studies indicate that this implementation, for which analytical energy gradients have been derived,[19] provides an accurate estimate of solvent effect on bright transitions and reliable excited state equilibrium geometries. However, it does not treat accurately electronic transition involving large electron density shifts and underestimates the stability of excited states with very large dipole moments (as the CT state).[20] We have thus recently developed a State Specific (SS) implementation of PCM/TD-DFT.[20,21] In SS approaches a fully variational formulation of solvent effects on the excited state properties is achieved, by solving a different effective Shroedinger equation for each state of interest and thus providing a more balanced description of solvent effects on different excited electronic states.

2 Evaluating the reliability of our computational approach

2.1 The model

Before starting the analysis of our results, it is important to verify not only the reliability of our computational approach but also the suitability of the model studied for interpreting the excited state dynamics in A-T DNA. On this respect our study of the absorption spectra[22] provides encouraging indications. Indeed, we have shown that computed absorption spectra and the excited state properties spectra does not significantly change when the phosphoribose backbone is included in the calculations and that in the FC region the orbitals involved in the electronic transitions are localized on the nucleobases.[22] Furthermore, when compared to the spectra of the monomers, (9Me-A)$_2$·(1Me-T)$_2$ exhibits all the most relevant features (vide infra) exhibited by the A-T DNA spectra.[23,24]

From the experimental point of view, Kohler et al. have shown[25] that the ground-state recovery of the long-living states does not depend on the number of the stacked bases,[25] confirming that the excimers involve two stacked bases, and that, on this respect, most of the main effects modulating the excited state decay of DNA are already operative in a tetramer.

2.2 The density functionals

As a first step we analyze the reliability of our computational approach in describing the absorption and emission properties of the bright states of adenine and thymine derivatives. For what concerns the insulated monomers, several studies indicate that PCM/PBE0 calculations provides Vertical Excitation and Emission Energies very close to the experimental band maxima[26] (within 0.15 eV) both for thymine[27−32] and for adenine [32−34]. Our computational results in the gas phase[29,34] are also in good agreement with those obtained by using sophisticated post-HF methods.[35−36]

Actually, a thorough comparison of the performances of different DF in the

computation of the absorption spectra of several classes of organic dyes shows that PBE0 exhibits a mean absolute error of only 22 nm.[12]

When employed in the study of stacked adenine oligomers [32−34] or in hydrogen bonded Ade-Thy tetramers [22] PCM/TD-PBE0 and PCM/TD-M052X calculations reproduce the most significant differences between the absorption spectra of the oligomers and that of the monomer:[37−41] a small blueshift and a remarkable decrease of the intensity of the band maximum, together with a small intensity increase of the band redwing. The very good agreement between the computed absorption spectra of $(dT)_2 \cdot (dA)_2$ and the experimental absorption spectra of DNA provides another decisive support to the reliability of our calculations for the study of the bright states of DNA tetramer. In fact, we predict that the formation of the double helix leads to a weak blue shift of the band maximum, a marked decrease of the absorption intensity and a noticeable shoulder in the low energy side. Furthermore, the absorbing states are delocalized in the two strands. All the above conclusions are fully confirmed by the experimental results.[23,24] The computed band maximum for $(9Me\text{-}A)_2 \cdot (1Me\text{-}T)_2$ is also very close to the experimental one of A-T DNA, with a difference in the range 0.20-0.25 eV, depending on the adopted basis set.[22]

For what concerns the localized dark states (for example those with n$\rightarrow\pi^*$ character), our computational approach provides results in good agreement with those obtained by using CASPT2 method both on thymine and adenine derivatives.[35−36] Furthermore it has successfully predicted [27,28] the involvement of a dark state, with $n \rightarrow \pi^*$ character, in the pyrimidine excited state dynamics, which has been confirmed also by experiments.[42]

It is instead necessary to discuss in detail, as already done in the main text of the paper, the PCM/TD-PBE0 description of the excited states with CT character. It is indeed well known that the energy of long range CT transitions can be severely underestimated by 'standard' density functionals, especially in the case of zero-overlap between the MO's of the donor and the acceptor molecule.[43] We have already examined in detail the case of the CT transitions between two stacked nucleobases [33−34]. In some cases 'standard' TD-DFT (as TD-PBE0) can provide a fairly accurate description also of the excited states with partial

CT character, as shown in the study of two stacked cytosine molecules [44]. For what concerns instead stacked adenine molecules, TD-PBE0 overestimates the stability of the CT transition with respect to other density functionals specifically designed for a suitable treatment of long range charge transfer transitions (M052X, LCωPBE [45], CAM-B3LYP [4] but the amount of the overestimation is not dramatic ($\sim$ 0.5 eV). The molecular orbitals of two stacked aromatic molecules with a inter-ring distance of $\sim$ 3.5 $\mathring{A}$ are significantly mixed, especially in the case of 'face to face' arrangement, explaining the relatively good performances of TD-PBE0. In any case the above studies highlight the importance of a correct treatment of solvent effects when calculating the energy of CT transitions, indicating that LR-PCM underestimates the stability of CT states with respect to SS-PCM calculations.[20,21] On the balance LR-PCM/TD-PBE0 calculations provide a good estimate of the energy of the CT state involving a stacked adenine dimer in aqueous solution, but this result is due to error compensation: PBE0 overestimates the stability of S_{CT} by $\approx$ 0.5 eV but, on the same time, LR-PCM underestimates its stability to a similar extent.

Another very recent study of Adenine stacked dimer provides similar indications [48] on the possible overstabilization of CT transitions by TD-PBE0. The importance of suitable long-range corrections (ruled by a parameter, μ) in the adopted density functional is demonstrated, as well as the relevance of a proper inclusion of environmental effects. On the other hand, it is comforting that in water solution, when assigning to μ a value that enables the density functional to provide a Vertical Excitation Energy of the Adenine bright state in agreement with the experimental absorption maximum, S_{CT} is predicted to be as stable as the spectroscopic states in the FC region.

On the ground of the above considerations, we can expect that TD-PBE0 delivers less accurate results when treating the CT transition involving a hydrogen bonded dimer, since in this case the overlap between the MO of the two nucleobases is nearly vanishing. In fact, as shown in Table 2 of the main text and in Table S1, TD-PBE0 remarkably overestimates the relative stability of CT transitions in adenine-thymine and cytosine-guanine Watson and Crick hydrogen bonded pairs.[46,47] In the former system, which is more relevant for

our present study, the relative stabilization with respect to the bright states is $\sim$ 1.3 eV larger than that obtained by CC/MP2 calculations. On the other hand, TD-M052X and TD-CAM-B3LYP results are in good agreement with those provided by post-HF calculations, without any dramatic overstabilization of the CT transitions. The residual difference is at least partially due to the different examined species (post-HF calculations where run on the un-substituted nucleobases while we considered the methylated compounds). For what concerns Ade-Thy pair (see Table 2 of the main text), the system investigated in the present study, not only TD-M052X and TD-CAM-B3LYP correctly predicts the relative stability of the Ade→Thy CT transition with respect to the bright states localized on the nucleobases (SB-Ade and SB-Thy), but there is a good quantitative agreement with CC2/MP2 calculations.[46] For what concerns instead the GC pair, TD-M052X predicts that the Gua→Cyt CT transition is more stable by $\approx$ 0.4 eV than the bright state localized on the monomers. CASPT2 results would indicate instead that the CT state is essentially degenerate with the lowest locally excited state, since the relative stability depends on the adopted equilibrium geometry.[47] Furthermore our study of stacked adenine dimers [33] shows that TD-M052X and TD-CAM-B3LYP picture agree with that provided by another density functional that have been purposely tailored for correctly describing long range CT, i.e. LC-ωPBE [45].

2.3 The solvent model

A detailed discussion on the advantages and the drawbacks of the different approaches for including solvent effects on the computed absorption and fluorescence spectra, it is obviously outside the scope of the present study.[6] Purely 'supramolecular' approaches, based on the inclusion of a large number of solvent molecules, suffer from severe limitations. Indeed very long simulation time and very accurate statistical sampling are necessary to reproduce bulk solvent effect on spectroscopic properties. Furthermore, when using classical molecular dynamics simulations to perform the averaging of the different solvent configurations, it is necessary to carefully check the reliability of the underlying force field in correctly describing the geometry of the first solvation shell and the en-

ergetic stability of the different possible configurations. Finally, when studying fluorescence spectra, it is necessary to properly describe dynamical solvent effect and, thus, the dynamic response of the solute-solvent degreesof freedom to the changes in the electronic density of the photoexcited solute. This task not only requires an 'ad hoc' parametrization procedure of the force field but also the use of very 'sophisticated' force fields, including, for example, atomic polarizability.

Summarizing the results of this section, the reliability of LR-PCM/TD-PBE0 calculations in the study of the bright states of DNA components in aqueous solution can be considered definitively assessed. The electronic transitions with CT character are instead significantly overstabilized by TD-PBE0, especially in the case of the hydrogen bonded dimer. On the other hand, SS-PCM/TD-DFT calculations are necessary to correctly describe solvent effects on the CT transitions. We thus resort to SS-PCM/TD-M052X and SS-PCM/TD-CAM-B3LYP calculations to obtain a reliable estimate of the relative stability of CT states with respect to locally excited electronic states.

According to the results discussed above, and on the ground of the considerations reported in the main text, it is clear that all the main conclusions of our manuscript (localization of the bright excited states, T1-S_B-min being predicted the lowest energy brigh excited state minimum and AA_{CT}-min the absolute excited state minimum) are well within the confidence range of our computational approach in the study of Ade-Thy tetramer.

3 Absorption spectra of the monomer

3.1 Thymine

The two lowest energy transitions of thymine derivatives fall at $\approx$ 5 eV and exhibit different features. Confirming previous computational analysis,[27−32] one state is almost dark and has a predominant n/π^* character, involving the transfer of an electron from a Kohn-Sham (KS) orbital corresponding to the Lone Pair of the C4-O8 carbonyl group towards a π^* orbital of the ring (hereafter Sn). For thymine this transition mainly corresponds to a HOMO-1→LUMO

excitation. The other transition (hereafter SB_T) is bright and it has π/π^* character, since can be described as an excitation from the highest energy π orbital of the ring to π^*. In thymine this transition corresponds to the HOMO→LUMO excitation. A schematic picture of the above orbitals can be found in Figure. 1.

3.2 Adenine

In agreement with previous CASPT2 studies on adenine[36], three electronic transitions contribute to the lowest energy absorption band, two with π/π^* character (usually labeled π^*L_a and π^*L_b, respectively, hereafter simply SB_A and L_b) and one with n/π^* character (hereafter Sn). Most of the absorption intensity is carried by the spectroscopic SB_A state, which corresponds essentially to the transition from the highest energy π occupied molecular orbital the lowest energy π^* molecular orbital (see Figure 1). For adenine those orbitals actually correspond to the HOMO and the LUMO, respectively. On the contrary the L_b state corresponds mainly to a HOMO→LUMO+1 transition. Finally, the Sn transition involves the transfer of an electron from a non bonding KS orbital to the π^* orbital (Sn). For adenine it corresponds to an HOMO-1→LUMO transition.

Table S1: Vertical excitation energies (in eV) computed for (1Me-Cyt)·(9Me-Gua) hydrogen bonded dimers (Watson and Crick pairing) in the gas phase. Oscillator strengths are given in parentheses.

	PBE0	M052X	CAM-B3LYP	CASPT2/MP2[a]	CASPT2/CIS[a]
GC CT	3.61(0.00)	5.00(0.00)	4.98(0.00)	4.75	4.2
SB-Cyt	5.02(0.06)	5.44(0.10)	5.32(0.10)	4.67	
Sb-Gua	4.94(0.10)	5.37(0.08)	5.27(0.07)	4.35	4.6

Cyt-Gua dimer ref. [47]

Table S2: Main features of the lowest energy excited states of of (9Me-A)$_2$·(1Me-T)$_2$ in their respective minima. PCM/TD-PBE0/6-31G(d) calculations on LR-PCM/TD-PBE0/6-31G(d) optimized geometries in aqueous solution. Relative Energies in eV with respect to the ground state minimum. The energies corrected[e] for the overestimation of the stability of CT transitions are reported in bold

Description	AT_{CT}[a]	AA_{CT}	A1-S_B	T1-S_B planar[b]	T1-S_B [c]
	LR-PCM results				
Osc. Strenght	.01	0.00	0.35	0.19	0.19
Energy (eq)	4.05	4.44	4.72	4.64	4.60
Energy (neq)	4.05 **5.05**	4.45 **5.15**	4.82	4.72	4.67
vee[d]	3.23 **4.23**	3.87 **4.56**	4.35	4.17	3.79
μ (debye)	20.2	16.8	3.3	4.00	3.8
			$\mathbf{Q}_m$		
1Me-T_1	-0.83	0.04	-0.09	-0.14	-0.16
1Me-T_2	-0.02	-0.04	-0.01	0.10	0.13
9Me-A_1	0.85	0.91	0.10	0.00	0.02
9Me-A_2	0.00	-0.91	0.00	0.04	0.01
			$\mathbf{v}_m$		
1Me-T_1	0.90	0.05	0.09	0.41	0.38
1Me-T_2	0.10	0.03	0.01	0.10	0.14
9Me-A_1	0.90	0.93	0.34	0.01	0.02
9Me-A_2	0.10	0.93	0.02	0.04	0.01
	SS-PCM results				
Osc. Str.	.01	0.00	0.20	0.10	0.07
Energy (neq)	3.58 **4.58**	3.75 **4.44**	4.85	4.82	4.83
vee[d]	2.76 **3.76**	3.17 **4.17**	4.49	4.34	4.06
μ	16.7	14.5	5.5	4.1	3.7

Notes: Energy of the ground state minimum: -1998.03619 a.u. a) Optimization Stopped because H transfer is happening. b)Pseudo Planar minimum. c) Starting from the the M052X minimum, non planar, decays to a CT state d) vertical emission energy. Non equilibrium solvent effect on the ground state are not considered e) The overestimation of CT states is corrected by comparing the relative stability of the CT states and A_1A_2-SB[i] state predicted by LR-PCM/TD-PBE0/6-31G(d) and LR-PCM/TD-M052X/6-31G(d) calculations.

Table S3: Main features of the lowest energy excited states of the (9Me-A)$_2$·(1Me-T)$_2$ in their respective minima. LR-PCM/TD-M052X/6-31G(d) calculations on LR-PCM/TD-PBE0/6-31G(d) optimized geometries. Relative Energies in eV with respect to the ground state minimum

Description	AT_{CT}[a]	AA_{CT}	A1-S_B	T1-S_B planar[b]
	LR-PCM results			
Energy (eq)	5.30	5.40	4.99	4.88
Energy (neq)	5.31	5.41	5.11	4.97
vee[c]	4.42	4.80	4.58	4.34
μ	16.00	15.3	5.8	5.1
	$\mathbf{Q}_m$			
1Me-T_1	-0.72	0.03	0.00	0.01
1Me-T_2	-0.02	-0.05	-0.01	-0.03
9Me-A_1	0.74	0.80	0.01	0.00
9Me-A_2	0.00	-0.83	0.00	0.02
	$\mathbf{v}_m$			
1Me-T_1	0.85	0.04	0.00	0.40
1Me-T_2	0.08	0.03	0.00	0.03
9Me-A_1	0.77	0.88	0.33	0.02
9Me-A_2	0.08	0.84	0.01	0.00
	SS-PCM results			
Osc. Str.	0.01	0.00	0.26	0.14
Energy (neq)	4.84	4.72	5.16	5.07
vee[b]	3.96	4.11	4.75	4.52
μ	16.3	14.4	5.6	5.0

Notes: Energy of the ground state minimum: -2000.04803192 a) Optimization Stopped because H transfer is happening. Planar minimum. b) vertical excitation energy. Non equilibrium solvent effect on the ground state are not considered

Table S4: Main features of the lowest energy excited states of the (9Me-A)$_2$·(1Me-T)$_2$ in their respective minima. LR-PCM/TD-CAM-B3LYP/6-31G(d) calculations on LR-PCM/TD-PBE0/6-31G(d) optimized geometries. Relative Energies in eV with respect to the ground state minimum

Description	AT_{CT}[a]	AA_{CT}	A1-S_B	T1-S_B planar[b]	T1-S_B[c]
	LR-PCM results				
Osc. Str.	0.04	0.00	0.32	0.17	0.15
Energy (neq)	5.30	5.36	5.02	4.87	4.83
vee[b]	4.43	4.75	4.62	4.35	4.00
μ	16.1	15.8	5.77	4.80	4.3
	SS-PCM results				
Osc. Str.	0.00	0.00	0.25	0.13	0.12
Energy (neq)	4.86	4.68	5.06	4.96	4.92
vee[b]	3.98	4.06	4.66	4.44	4.08
μ	16.3	14.4	5.56	4.78	3.3

Notes: Energy of the ground state minimum: -1999.32030915 a) Optimization Stopped because H transfer is happening. Planar minimum. b) vertical excitation energy. Non equilibrium solvent effect on the ground state are not considered c) Starting from the the M052X minimum, corresponding to the 6th column of Table S2

Table S5: Main features of the lowest energy excited states of (9Me-A)$_2$·(1Me-T)$_2$ in their respective minima. PCM/TD-M052X/6-31G(d) calculations on LR-PCM/TD-M052X/6-31G(d) optimized geometries. Relative Energies in eV with respect to the ground state

	Description	AT_{CT}[a]	AA_{CT}	A1-S_B	T1-S_B
		LR-PCM results			
	Osc. Strenght	0.08	0.03	0.443	0.242
	Energy (eq)	5.37	5.29	4.94	4.75
	Energy (neq)	5.38	5.29	5.05	4.82
	vee[c]	4.41	4.59	4.43	3.80
	μ	16.0	9.7	3.90	3.5
		$\mathbf{Q}_m$			
	1Me-T_1	-0.72	0.01	-0.02	-0.01
	1Me-T_2	-0.02	-0.05	-0.02	-0.03
minimum	9Me-A_1	0.74	-0.59	0.03	0.02
	9Me-A_2	0.00	0.62	0.01	0.02
		$\mathbf{v}_m$			
	1Me-T_1	0.85	0.02	0.01	0.30
	1Me-T_2	0.08	0.02	0.01	0.02
	9Me-A_1	0.77	0.64	0.25	0.01
	9Me-A_2	0.08	0.62	0.03	0.01
		SS-PCM results			
	Osc. Str.	0.01	0.00	0.23	0.12
	Energy (neq)	4.91	4.84	5.09	4.90
	vee[c]	3.96	4.13	4.59	3.98
	μ	16.3	10.7	4.6	4.5

Notes: Energy of the ground state minimum: -2000.05063774 a) Optimization Stopped because H transfer is happening. b) Optimization goes to A_1-S_B c) vertical excitation energy. Non equilibrium solvent effect on the ground state are not considered

References

[1] (a) Adamo, C.; Barone, V. *J. Chem. Phys.* **1999** *110*, 6158-6170. (b) Enzerhof, M.; Scuseria, G.E. *J. Chem. Phys.* **1999**, *110*, 5029. (c) Adamo, C.; Scuseria, G.E.; Barone, V. *J. Chem. Phys.* **1999**, *111*, 2889-2899.

[2] Adamo, C., Scuseria, G.E. & Barone, V. *J. Chem. Phys.* **111,** 2889 (2000).

[3] Zhao, Y.; Schultz, N.E.; Truhlar, D.G. *J. Chem. Theory Comput.* **2006** *2* 364.

[4] (a) Yanai, T., Tew, D.B.& Handy, N.C. *Chem. Phys. Lett.*, **393,** 51 (2004).

[5] (a) Yanai, T.; Tew, D.P.; Handy, N.C. *Chem. Phys. Lett.* **2004**, *393* 51-55. (b) Tawada, Y., Tsuneda, T., Yanagisawa, S., Yanai, T.& Hirao K. *J. Chem. Phys.*, **2004**,*120*, 8425.

[6] (a) Miertus, S., Scrocco, E.& Tomasi, J. *Chem. Phys* **1981***55* 117. (b Tomasi, J.; Mennucci, B.; Cammi, R. *Chem. Rev.* **2005**, *105*, 2999-3094.

[7] Cossi, M.; Rega, N.; Scalmani, G.; Barone, V. *J. Chem. Phys.* **2001**, *114* 5691

[8] Gaussian Development Version, Revision F.02, M. J. Frisch, G. W. Trucks, H. B. Schlegel, G. E. Scuseria, M. A. Robb, J. R. Cheeseman, J. A. Montgomery, Jr., T. Vreven, G. Scalmani, B. Mennucci, V. Barone, G. A. Petersson, M. Caricato, H. Nakatsuji, M. Hada, M. Ehara, K. Toyota, R. Fukuda, J. Hasegawa, M. Ishida, T. Nakajima, Y. Honda, O. Kitao, H. Nakai, X. Li, H. P. Hratchian, J. E. Peralta, A. F. Izmaylov, K. N. Kudin, J. J. Heyd, E. Brothers, V. Staroverov, G. Zheng, R. Kobayashi, J. Normand, J. L. Sonnenberg, S. S. Iyengar, J. Tomasi, M. Cossi, N. Rega, J. C. Burant, J. M. Millam, M. Klene, J. E. Knox, J. B. Cross, V. Bakken, C. Adamo, J. Jaramillo, R. Gomperts, R. E. Stratmann, O. Yazyev, A. J. Austin, R. Cammi, C. Pomelli, J. W. Ochterski, P. Y. Ayala, K. Morokuma, G. A. Voth, P. Salvador, J. J. Dannenberg, V. G. Zakrzewski, S. Dapprich, A. D. Daniels, M. C. Strain, O. Farkas, D. K. Malick, A. D. Rabuck, K. Raghavachari, J. B. Foresman, J. V. Ortiz, Q. Cui, A. G. Baboul, S. Clifford, J. Cioslowski, B. B. Stefanov, G. Liu, A.

Liashenko, P. Piskorz, I. Komaromi, R. L. Martin, D. J. Fox, T. Keith, M. A. Al-Laham, C. Y. Peng, A. Nanayakkara, M. Challacombe, W. Chen, M. W. Wong, and J. A. Pople, Gaussian, Inc., Wallingford CT, 2006.

[9] (a) Improta, R.; Benzi, C.; Barone, V. *J. Am. Chem. Soc.* **2001***123* 12568. (b) Improta, R.; Barone, V.; Kudin, K.N.; Scuseria, G.E. *J. Am. Chem. Soc.* **2001***123* 3311. (c) Improta, R.; Mele, F.; Crescenzi, O.; Benzi, C.;Barone, V. *J. Am. Chem. Soc.* **2002***124* 7857. (d) Langella, E.; Improta, R.; Barone, V. *J. Am. Chem. Soc* **2002**,*124* 11531

[10] (a) Improta, R.; Santoro, F.; Dietl, C.; Papastathopoulos, E.; Gerber, G. *Chem. Phys. Lett.* **2004**, *387* 509; (b) Sanna, N. *et al. J. Am. Chem. Soc.* **2005**, **127** 15429.

[11] Zhao, Y. & Truhlar, D.G. *J. Chem. Theory. Comput.* **1,** 415 (2005).

[12] Jacquemin, D.; Perpete, E.A.; Ciofini, I.; Adamo, C. *Acc. Chem. Res.* **2009**, *42*, 326334

[13] Barone, V.; Improta, R.; Rega, N. *Acc. Chem. Res.* **2008**, *41*, 605?616

[14] Improta, R.; Barone, V; Santoro, F. *Angew. Chem., Int. Ed.* **2007**, *46*, 405?408

[15] Improta, R.; Barone, V; Santoro, F. *J. Phys. Chem. B* **2007**, *111*, 14080-14082

[16] Zhao, Y.; Truhlar, D.G. *Acc. Chem. Res.* **2008** *41*, 157-167.

[17] Barone, V.; Cossi, M.; Tomasi, J. *J. Chem. Phys.* **1997**, *107* 3210.

[18] Cossi, M. & Barone, V. *J. Chem. Phys.* **115,** 4708-4717 (2001).

[19] Scalmani, G.; Frisch, M.J.; Mennucci, B.; Tomasi, J.; Cammi, R.; Barone, V. *J. Chem. Phys.* **2006**, *124*, 094107.

[20] Improta, R.; Barone, V.; Scalmani, G.; Frisch, M. J. *J. Chem. Phys.* **2006**, *125*, 054103

[21] Improta, R.; Frisch, M.J.; Scalmani, G.; Barone, V. *J. Chem. Phys.* **2007**, *127*, 74504.

[22] Santoro, F.; Barone, V.; Improta, R. *Chem.Phys.Chem.* **2008** *9*, 2531-2537.

[23] Onidas, D.; Gustavsson, T.; Lazzarotto, E.; Markovitsi, D. *J. Phys. Chem. B* **2007**, *111*, 9644-9650.

[24] Markovitsi, D.; Gustavsson, T.; Talbot, F. *Photochem., Photobiol. Sci.* **2007**, *6*, 717.

[25] Takaya, T.; Su, C.; de La Harpe, K.; Crespo-Hernńdez, C.E.; Kohler, B. *Proc. Nat. Acad. Sci.* **2008**, *105*, 10285-10290.

[26] Crespo-Hernandez, C.E.; Cohen, B.; Hare, P.M.; Kohler, B. *Chem. Rev.* **2004** *104*, 1977-2020.

[27] Santoro, F.; Barone, V.; Gustavsson, T.; Improta, R. *J. Am. Chem. Soc.* **2006**, *128*, 16312-16322.

[28] Gustavsson, T.; Sarkar, N.; Lazzarotto, E.; Markovitsi, D.; Barone, V.; Improta, R. *J. Phys. Chem. B* **2006**, *J 110*, 12843?12847

[29] Gustavsson, T.; Banyasz, A.; Lazzarotto, E.; Markovitsi, D.; Scalmani, G.; Frisch, M. J.; Barone, V.; Improta, R. *J. Am. Chem. Soc.* **2006**, *128*, 607-619.

[30] Gustavsson, T.; Sarkar, N.; Lazzarotto, E.; Markovitsi, D.; Improta, R. *Chem. Phys. Lett.* **2006** *429* 551.

[31] Improta, R.; Barone, V. *J. Am. Chem. Soc.* **2004**, *126* 14320

[32] Improta, R.; Barone, V. *Theor. Chem. Acc.* **2008**, *120*, 491.

[33] Improta, R. *Phys. Chem. Chem. Phys.* **2008**, *10*, 2656-2664.

[34] Santoro, F.; Barone, V.; Improta, R. *Proc. Natl. Acad. Sci. U. S. A.* **2007** *104*, 9931-9937.

[35] (b) Serrano-Perez, J. J.; Gonzalez-Luque, R.; Merchan, M.; Serrano-Andres, L. *J. Phys. Chem. B* **2007** *111*, 11880-11883

[36] (a) Serrano-Andres, L.; Merchan, M.; Borin, A.C. *Proc. Nat. Acad. Sci.* **2006**, *103*, 8691-8696. (b) Serrano-Andres, L.; Merchan, M.; Borin, A.C. *Chem. Eur. J.* **2006**, *12*, 6559

[37] Crespo-Hernández, C.E.; Cohen, B.; Kohler, B. *Nature* **2005**, *436*, 1141-1144.; ibidem (2006) **441,** E8.

[38] Crespo-Hernandez, C. E.; Kohler, B. *J. Phys. Chem. B* **2004**, *108*, 11182?11188.

[39] Kwok, W.-M.; Ma, C.; Phillips, D.L. *J. Am. Chem. Soc.* **2006**, *128*, 11894-11905.

[40] Cohen, B.; Hare, P.M.; Kohler, B. *J. Am. Chem. Soc.* **2003** *125* 13594.

[41] Markovitsi, D.; Talbot, F.; Gustavsson, T.; Onidas, D.; Lazzarotto E.; Marguet, S. *Nature* **2006**, *441*, E7.

[42] Hare, P.M., Crespo-Hernandez, C.E.; Kohler, B. *Proc. Nat. Acad. Sci. U.S.A.* **2007**, *104*, 435-441.

[43] (a) Dreuw, A.; Head-Gordon, M. *Chem. Rev.* **2005**, *105*, 4009. (b) Wanko, M. *et al. J. Chem. Phys.* **2004**, *120* 1674.

[44] Santoro, F.; Barone, V.; Improta, R. *J. Comput. Chem.* **2008**, *29* 957.

[45] Vydrov, O.A.; Scuseria, G.E. *J. Chem. Phys.* **2006**, **125**, 234109.

[46] Perun, S.; Sobolewski, A.L.; Domcke, W. *J. Phys. Chem. A.* **2006**, *110* 9031

[47] Sobolewski, A.L.; Domcke, W. *Phys. Chem. Chem. Phys.* **2004**, **6**, 2763.

[48] Lange, A. W.; Rohrdanz, M. A.; Herbert, J. M. *J. Phys. Chem. B* **2008**, *112*, 6304.

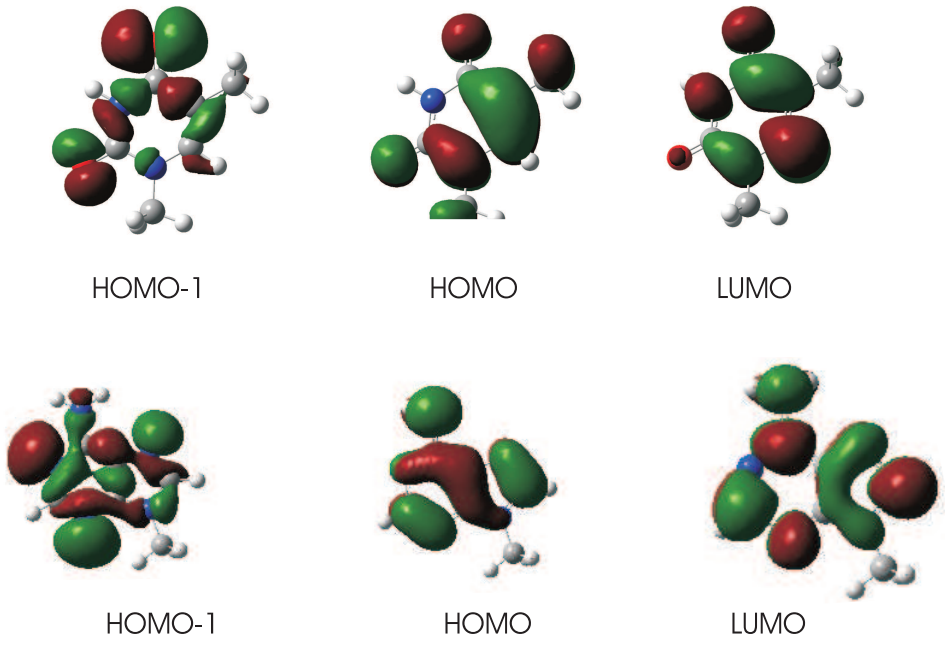

Figure 1: Schematic picture of the KS frontier orbitals of 1Me-Thy (up) and 9ME-Ade (bottom)

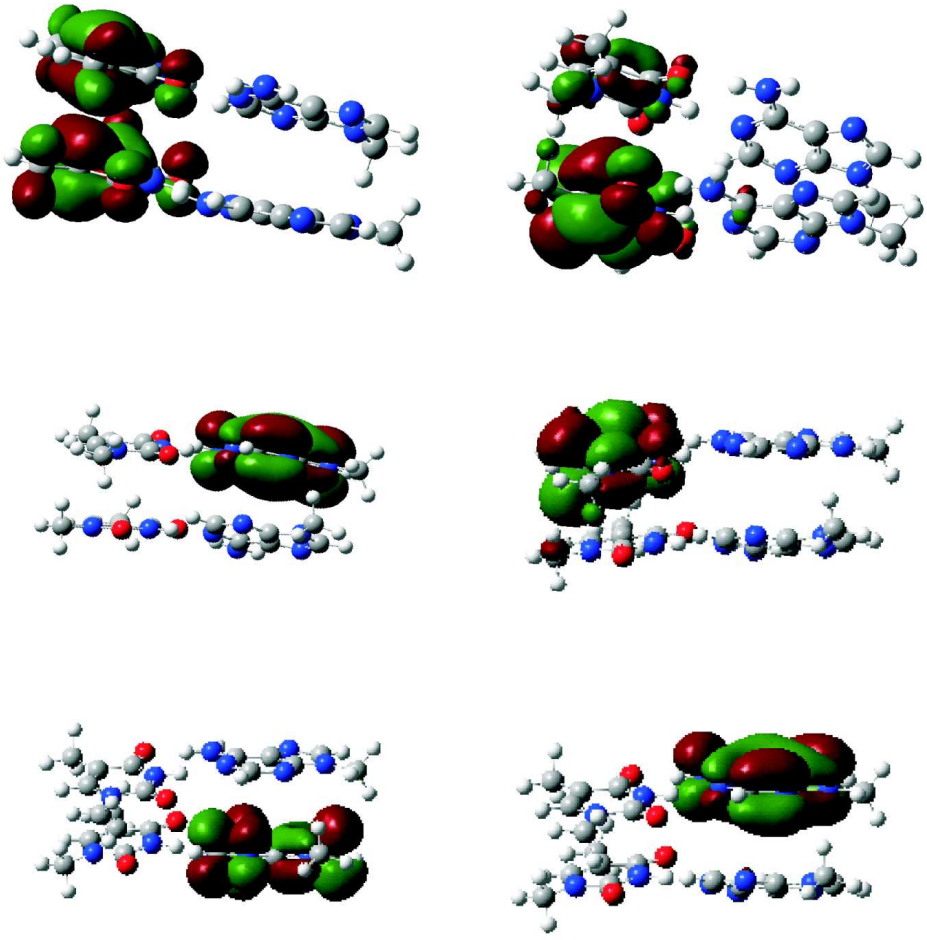

Figure 2: Schematic picture of the KS frontier orbitals involved in some relevant electronic transitions (see Figure 3 of the text) of (9Me-Ade)$_2$·(1Me-Thy)$_2$. Up: T_1T_2-SB^i in the FC region. Middle: AT_{CT} in AT_{CT}-min. Bottom: AA_{CT} in AT_{CT}-min. The electronic transition alsways involves mainly the excitation from the KS orbitals on the left towards those on the right.

Cartesian Coordinates of AT_{CT}-min, obtained at the LR-PCM/TD-PBE0/6-31G(d) level

Atom	X	Y	Z
N	3.273453	2.627019	1.303781
C	1.941907	2.349986	1.323089
N	1.610192	1.049600	1.571312
C	2.505782	-0.010330	1.895516
C	3.853987	0.318964	1.878341
C	4.249940	1.624216	1.544465
O	1.075790	3.217355	1.111312
O	1.983839	-1.152679	2.191487
C	3.684689	3.947315	0.897186
H	0.619874	0.837496	1.611600
C	4.887968	-0.713183	2.223158
H	5.269074	1.978545	1.618120
H	5.899615	-0.308889	2.104382
H	4.801490	-1.600597	1.584598
H	4.788989	-1.063003	3.260079
N	4.458768	-0.379219	-1.581316
C	3.202401	0.201130	-1.636416
N	2.158487	-0.686749	-1.524690
C	2.242753	-2.048337	-1.323000
C	3.584135	-2.583583	-1.224458
C	4.617954	-1.719278	-1.364988
O	3.040594	1.398251	-1.831772
O	1.221188	-2.745030	-1.263637
C	5.596976	0.517782	-1.687973
H	1.207807	-0.271859	-1.563631
C	3.759846	-4.046907	-0.979454
H	3.295701	-4.341228	-0.030686
H	3.280078	-4.640700	-1.766218
H	4.820396	-4.314211	-0.942339
H	5.653762	-2.056373	-1.316544
H	-0.443097	-2.148950	-1.778774
N	-1.357645	-1.781465	-2.060909
C	-1.605208	-0.476220	-1.905554
H	-2.141039	-2.423659	-2.123222
N	-0.576372	0.368499	-1.677787
C	-0.824132	1.671887	-1.486245
N	-1.998074	2.297168	-1.475478
C	-3.006850	1.445821	-1.713957
C	-2.902449	0.077107	-1.959844
N	-4.142906	-0.494346	-2.126673
C	-4.969095	0.505547	-1.938865
N	-4.352607	1.708565	-1.715197
H	-6.052347	0.445493	-2.015868
C	-4.978460	2.978781	-1.418694
H	0.055189	2.282082	-1.289024
H	0.557126	-1.617322	2.033129
H	-0.668765	-2.951543	1.938600
N	-0.472782	-1.947465	1.930289
C	-1.483995	-1.122834	1.833089
N	-1.238158	0.219621	1.817820
C	-2.220772	1.068764	1.672892
N	-3.553444	0.792695	1.521473
C	-3.793752	-0.487553	1.538725
C	-2.849595	-1.544342	1.709266
N	-3.452378	-2.736064	1.705864
C	-4.745381	-2.445731	1.490413
N	-5.002622	-1.128827	1.398167
H	-1.958193	2.124438	1.656446
H	-5.531673	-3.192779	1.417894
C	-6.298037	-0.488464	1.228545
H	-6.146829	0.589114	1.288085
H	-6.717380	-0.750949	0.256021
H	-6.971820	-0.807499	2.025226
H	-4.466259	3.772440	-1.966797
H	-6.022953	2.940072	-1.733340
H	-4.925964	3.190975	-0.346996
H	6.512964	-0.072804	-1.624197
H	5.570516	1.049139	-2.643446
H	5.563385	1.243895	-0.869952
H	4.745234	4.072256	1.130712
H	3.542510	4.096735	-0.181108

Cartesian Coordinates of AA_{CT}-min obtained at the LR-PCM/TD-PBE0/6-31G(d) level

Atom	X	Y	Z
N	3.289780	2.691501	1.144061
C	1.941483	2.412460	1.248170
N	1.655458	1.109791	1.583842
C	2.551622	0.108924	1.884552
C	3.945977	0.483153	1.823377
C	4.237713	1.753414	1.443753
O	1.075104	3.250023	1.044637
O	2.153655	-1.028249	2.183700
C	3.650994	4.020299	0.675342
H	0.654142	0.872011	1.622214
C	4.983708	-0.531978	2.180155
H	5.268907	2.100476	1.372348
H	5.991043	-0.124978	2.053067
H	4.885234	-1.426418	1.555441
H	4.872839	-0.856989	3.221311
N	4.330549	-0.460977	-1.638904
C	3.061144	0.095940	-1.638657
N	2.038072	-0.787549	-1.404044
C	2.161734	-2.137450	-1.128580
C	3.520075	-2.650351	-1.095647
C	4.528221	-1.789113	-1.366519
O	2.884538	1.291939	-1.845761
O	1.163459	-2.838967	-0.940732
C	5.443436	0.433389	-1.909939
H	1.055102	-0.399165	-1.493370
C	3.731997	-4.098114	-0.792867
H	3.338646	-4.350646	0.198695
H	3.202760	-4.731806	-1.513892
H	4.794963	-4.355179	-0.819719
H	5.568656	-2.113940	-1.383724
H	-0.601635	-2.302125	-1.753532
N	-1.449370	-1.961554	-2.209237
C	-1.657897	-0.600197	-1.922522
H	-2.243880	-2.520027	-1.902605
N	-0.593666	0.211781	-1.706005
C	-0.768036	1.512533	-1.506000
N	-1.948574	2.210252	-1.477211
C	-2.990343	1.385483	-1.718524
C	-2.949284	0.003921	-1.967825
N	-4.201370	-0.510692	-2.120651
C	-5.026863	0.524499	-1.899919
N	-4.316780	1.709678	-1.728778
H	-6.087514	0.543503	-2.121471
C	-4.864143	2.998738	-1.398890
H	0.134879	2.088795	-1.322464
H	0.547795	-1.586407	2.036657
H	-0.611013	-2.943565	1.976136
N	-0.435126	-1.935517	1.964190
C	-1.427841	-1.090409	1.842019
N	-1.147290	0.242866	1.804905
C	-2.123510	1.107274	1.650486
N	-3.461124	0.853384	1.533148
C	-3.727062	-0.422726	1.558066
C	-2.799557	-1.489381	1.733434
N	-3.419195	-2.672803	1.771504
C	-4.714491	-2.363172	1.577692
N	-4.949106	-1.045072	1.461498
H	-1.841289	2.156695	1.610801
H	-5.515487	-3.098714	1.533874
C	-6.233495	-0.388223	1.275413
H	-6.063208	0.687489	1.313559
H	-6.642346	-0.652398	0.299358
H	-6.914894	-0.685870	2.075419
H	-4.265182	3.781999	-1.870632
H	-5.890753	3.061940	-1.768663
H	-4.862902	3.165906	-0.315171
H	6.362749	-0.153216	-1.941183
H	5.296817	0.935710	-2.869157
H	5.522174	1.193766	-1.128007
H	4.729737	4.146306	0.778122
H	3.366280	4.132967	-0.374639

Cartesian Coordinates of A1-S_B-min obtained at the LR-PCM/TD-PBE0/6-31G(d) level

Atom	X	Y	Z
N	3.15373	2.69689	1.21735
C	1.81972	2.34749	1.27088
N	1.5791	1.0334	1.58627
C	2.5163	0.07098	1.91978
C	3.89029	0.50865	1.88993
C	4.14103	1.79784	1.53301
O	0.92376	3.14984	1.03201
O	2.15583	-1.07993	2.22146
C	3.46788	4.04051	0.76339
H	0.5769	0.7646	1.6464
C	4.96567	-0.45953	2.26656
H	5.1552	2.19412	1.49781
H	5.95592	-0.00283	2.17731
H	4.93301	-1.35003	1.62881
H	4.83996	-0.80648	3.29919
N	4.45652	-0.37403	-1.54643
C	3.17789	0.15111	-1.62069
N	2.1693	-0.76872	-1.46968
C	2.30712	-2.1256	-1.25072
C	3.67091	-2.60599	-1.14977
C	4.67019	-1.70669	-1.31323
O	2.97278	1.34324	-1.81338
O	1.31391	-2.85625	-1.1649
C	5.55942	0.55711	-1.72001
H	1.19939	-0.39191	-1.54675
C	3.90351	-4.05961	-0.89287
H	3.4526	-4.36458	0.05852
H	3.44344	-4.67545	-1.67422
H	4.97298	-4.28637	-0.85751
H	5.71776	-2.0049	-1.27023
H	-0.40242	-2.30513	-1.65757
N	-1.32687	-1.9629	-1.93337
C	-1.57738	-0.64893	-1.87108
H	-2.10825	-2.61007	-1.90947
N	-0.54614	0.2101	-1.72228
C	-0.79097	1.52585	-1.64542
N	-1.96138	2.15322	-1.69879
C	-2.97176	1.28546	-1.84698
C	-2.87364	-0.10097	-1.96251
N	-4.11787	-0.67896	-2.07937
C	-4.9379	0.34188	-2.00628
N	-4.31431	1.55605	-1.89249
H	-6.02143	0.28038	-2.0782
C	-4.9329	2.8455	-1.68444
H	0.09174	2.14929	-1.51535
H	0.43692	-1.67287	2.09992
H	-0.78956	-2.95734	2.10061
N	-0.55357	-1.96595	2.10107
C	-1.51123	-1.04875	1.92296
N	-1.18304	0.24353	1.82782
C	-2.12735	1.16218	1.57461
N	-3.50772	0.91958	1.47345
C	-3.79499	-0.34732	1.52144
C	-2.89499	-1.4363	1.76965
N	-3.54197	-2.59521	1.91064
C	-4.84243	-2.29327	1.68844
N	-5.04259	-0.95248	1.47548
H	-1.80031	2.18621	1.43699
H	-5.65791	-3.01008	1.68558
C	-6.30135	-0.28524	1.26579
H	-6.11095	0.78904	1.22812
H	-6.76201	-0.60521	0.3244
H	-6.98888	-0.49968	2.09119
H	-4.40827	3.60147	-2.27298
H	-5.97505	2.79665	-2.00683
H	-4.88829	3.1187	-0.62537
H	6.49646	0.00056	-1.67249
H	5.47981	1.05904	-2.6875
H	5.54126	1.31298	-0.93083
H	4.53315	4.22106	0.91548
H	3.22813	4.14265	-0.29929

Cartesian Coordinates of T1-S_B-min obtained at the LR-PCM/TD-PBE0/6-31G(d) level

Atom	X	Y	Z
N	3.09552	2.4965	1.54091
C	1.76471	2.10712	1.52622
N	1.50406	0.77889	1.64691
C	2.46416	-0.20684	1.97245
C	3.81253	0.23059	1.97359
C	4.14172	1.58543	1.65891
O	0.86411	2.94186	1.38574
O	2.07223	-1.38268	2.20545
C	3.42368	3.85541	1.19282
H	0.5019	0.51555	1.70332
C	4.89134	-0.73882	2.28861
H	5.10372	2.02148	1.9242
H	5.87858	-0.33894	2.0373
H	4.73362	-1.67993	1.74819
H	4.8951	-1.00086	3.35891
N	4.51019	-0.12216	-1.60671
C	3.21269	0.37676	-1.62435
N	2.22796	-0.57542	-1.61713
C	2.39667	-1.93991	-1.49442
C	3.77243	-2.3922	-1.39401
C	4.75495	-1.45576	-1.46073
O	2.98451	1.57897	-1.65903
O	1.42483	-2.70102	-1.48736
C	5.57627	0.86038	-1.51815
H	1.24711	-0.21456	-1.64647
C	4.03839	-3.8503	-1.22784
H	3.59835	-4.21946	-0.29326
H	3.581	-4.42702	-2.04015
H	5.11194	-4.05758	-1.21204
H	5.80833	-1.73177	-1.40679
H	-0.33821	-2.12938	-1.92746
N	-1.26853	-1.76542	-2.14645
C	-1.51573	-0.46454	-1.95419
H	-2.04775	-2.41596	-2.1662
N	-0.47915	0.37408	-1.74015
C	-0.71265	1.67612	-1.53557
N	-1.88073	2.31061	-1.5107
C	-2.89635	1.46737	-1.73364
C	-2.81101	0.09535	-1.97915
N	-4.05706	-0.4543	-2.16281
C	-4.86889	0.56677	-2.01309
N	-4.23501	1.7533	-1.76307
H	-5.95134	0.52454	-2.10952
C	-4.84345	3.02661	-1.44907
H	0.17553	2.28015	-1.36043
H	0.31782	-1.93546	2.02065
H	-0.90141	-3.19961	1.87632
N	-0.67006	-2.21794	1.98457
C	-1.62375	-1.29754	1.82632
N	-1.27851	0.00949	1.84266
C	-2.22087	0.94805	1.69012
N	-3.52731	0.7858	1.51304
C	-3.85147	-0.51493	1.49413
C	-2.99391	-1.60243	1.6573
N	-3.68898	-2.79029	1.60548
C	-4.93158	-2.41849	1.39894
N	-5.09326	-1.06187	1.31988
H	-1.85409	1.97387	1.70869
H	-5.77968	-3.09176	1.30065
C	-6.33122	-0.33574	1.13785
H	-6.10141	0.73021	1.17926
H	-6.77625	-0.5733	0.16772
H	-7.04023	-0.58231	1.93315
H	-4.30594	3.82531	-1.96504
H	-5.88284	3.01606	-1.78338
H	-4.80606	3.20498	-0.36996
H	6.5354	0.34743	-1.6029
H	5.47241	1.5934	-2.32035
H	5.50469	1.37785	-0.55033
H	4.20264	4.22581	1.86942
H	3.81521	3.87129	0.1645